Food Chemistry 433 (2024) 137330

Contents lists available at ScienceDirect

Food Chemistry

journal homepage: www.elsevier.com/locate/foodchem

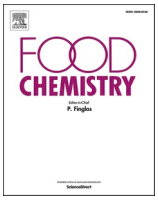

Characterization of Pickering emulsions stabilized by delipidated egg yolk granular protein nanoparticles crosslinked with ultraviolet radiation

Florencia Ridella, Ismael Marcet, Gemma Gutiérrez, Manuel Rendueles *, Mario Díaz

Department of Chemical and Environmental Engineering, University of Oviedo, C/ Julián Clavería 8, 33006 Oviedo, Spain

ARTICLE INFO

Keywords:
Egg yolk protein
Nanoparticle
Ultraviolet radiation
pH
Self-assembly
Emulsion microstructure

ABSTRACT

In this study, delipidated egg yolk proteins were used for the first time to prepare nanoparticles by the self-assembling method at pH 8.0, then treated with UV-C as a crosslinking agent, and their stability tested at pH 7.0, which is a more convenient pH for food applications. According to the results obtained, non-irradiated nanoparticles had a size of 431.8 ± 75.7 nm at pH 7.0, but the 10 min UV-C irradiated nanoparticles had an average size of 139.7 ± 5.9 nm. These nanoparticles also showed a high resistance to destabilization by SDS, urea or DTT and noticeable antioxidant and ferrous chelating activities. Pickering emulsions prepared at the nanoparticle concentration of 1 % (w/w) showed the smallest average droplet size and the lowest Turbiscan stability index value after 80 days of storage. All in all, these results have important implications for the utilisation of these proteins as a conventional Pickering emulsifying agent.

1. Introduction

Pickering emulsions are emulsions stabilized by micro- and nanoparticles that decrease the interfacial tension between immiscible phases, generally water and oil, stabilizing droplets, increasing functionality of emulsions and reducing toxicity compared with the use of surfactants (T. Zhang, Xu, Chen, Wang, Wang, & Zhong, 2021). For this purpose, many research studies have focused on preparing Pickering emulsions with solid inorganic or synthetic particles, such as SiO_2 or carbon nanotubes (Ning et al., 2020); however, these kinds of particles meet with certain disapproval in the food and pharmaceutical industries due to health concerns. As a result, nanoparticles prepared using food-grade biopolymers and acting as Pickering emulsifiers are attracting more attention for such applications, but not all biopolymers are suitable for preparing Pickering emulsifiers. In this respect, these particles must possess an intermediate level of hydrophobicity to be adsorbed at the interface between the two immiscible liquids and at the same time, remain insoluble in both phases during the lifetime of the emulsion.

A variety of food-grade biopolymers have been used in order to prepare Pickering emulsifying agents; in particular, protein-based particles have exceptional characteristics, such as their amphiphilic nature, low cost and environmentally friendly behaviour. Until now, different food-grade protein-based nanoparticles have been used as stabilizers in Pickering emulsions, including those prepared from tea protein (Ren et al., 2021), soy protein (Yang, Su, Meng, Zhang, Kennedy, & Liu, 2020), kafirin (Xiao, Gonzalez, & Huang, 2016), chitosan/collagen peptides (Sharkawy, Barreiro, & Rodrigues, 2021) and wheat protein (Zhu, Chen, McClements, Zou, & Liu, 2018). These protein-based nanoparticles can be stabilised by covalent bonds to achieve greater structural stability and be less sensitive to environmental changes. The most usual crosslinking methods found in the literature involve the use of heating, which produces an increase in the number of intraparticle disulphide bonds (Ning et al., 2020), or chemicals such as glutaraldehyde (Petker, Rogers, & Joye, 2021) or genipin (Lin et al., 2021), the former being a toxic compound that must be thoroughly removed from the reaction media and the latter a reagent that usually requires long reaction times in order to exert its effect. Another option in this regard, UV radiation, is an economical, non-thermal and environmentally friendly crosslinking agent that has been used by other authors in order to improve the mechanical and physical properties of protein-based films, such as those prepared with whey protein (Díaz, Candia, & Cobos, 2016) or peanut protein (Fathi, Almasi, & Pirouzifard, 2018), but its application to improve the stability of protein-based nanoparticles has not yet been evaluated.

Protein-based nanoparticles can be produced using a variety of methods aimed at reducing protein solubility. Among these, the pH-driven self-assembly method relies on the isoelectric point of proteins, since proteins near their isoelectric point tend to aggregate, forming

* Corresponding author.
E-mail address: mrenduel@uniovi.es (M. Rendueles).

https://doi.org/10.1016/j.foodchem.2023.137330
Received 27 October 2022; Received in revised form 8 June 2023; Accepted 28 August 2023
Available online 30 August 2023

compact structures (Tarhini, Greige-Gerges, & Elaissari, 2017). This versatile method can be customized for different protein systems, facilitating the production of nanoparticles with specific properties and functionalities (T. Zhang et al., 2021).

On the other hand, egg yolk can be easily separated into two fractions: egg yolk granules and plasma. The plasma fraction has a high lipidic content (73 %) and a low protein content (25 %) and shows emulsifying and gelling properties similar to those of the whole egg yolk (Kiosseoglou & Paraskevopoulou, 2005); however, the granular fraction has a low lipid content (31 %) and a high protein content (64 %), but these proteins are mostly insoluble in distilled water and are only properly solubilised in a solution with an NaCl concentration higher than 0.3 M. In this context, A. Wang, Xiao, Wang, Li, and Wang (2020) suggested that raw egg yolk granules can be used directly as a Pickering emulsifying agent. In addition, Y. Zhang, Chen, Xiong, Ding, Li, and Luo (2022) extracted high density lipoproteins from the granular fraction and prepared Pickering emulsions at several pH values and protein concentrations. Nevertheless, it must also be remembered that 65 % of the lipids found in the granular fraction are phospholipids, which constitute a valuable ingredient frequently used as an emulsifier, gelling agent and lubricant in different industries (H. Wang, Yao, & Wang, 2014). These valuable lipids can be extracted from the granular fraction using organic solvents such as ethanol, while the remaining highly denatured proteins show a very low water solubility, which limits their range of applications for the food industry. To date, these delipidated egg yolk granular proteins have been used to prepare edible films or microcapsules (Marcet, Sáez-Orviz, Rendueles, & Díaz, 2022), however, the potential of such delipidated and non-hydrolysed proteins for the preparation of protein-based nanoparticles has never been explored.

Consequently, the aim of this study was to characterize O/W Pickering emulsions prepared using nanoparticles formed with delipidated egg yolk granular proteins stabilised by UV-C. The size, morphology, antioxidant properties and intra-particle forces of the nanoparticles were assessed, and the rheological properties, microstructure and stability of the Pickering emulsions were also tested. To the best of our knowledge, this is the first study to investigate not only the self-assembly properties of the delipidated egg yolk granular proteins, but also the use of UV-C as a crosslinker of protein-based nanoparticles, testing them as a Pickering emulsifying agent.

2. Materials and methods

2.1. Obtaining delipidated proteins from egg yolk granules

Delipidated egg yolk granules were obtained as described by (Sáez-Orviz, Marcet, Rendueles, & Díaz, 2022). Briefly, the egg yolk was separated from the egg white manually and dried using blotting paper. The vitelline membrane was broken, and the liquid egg yolk was poured into a beaker and diluted with water to a proportion of 1:1.5 (w/w). The pH of the diluted egg yolk was adjusted to 7.0 with 0.1 mol/L NaOH and centrifuged for 45 min at 10,000 r/min. Then, the supernatant was discarded, and the pellet was recovered and lyophilized at 0.1 mBar, −70 °C for 24 h (Cryodos −80, Telstar, Spain). Afterwards, the sediment was delipidated with absolute ethanol (50:1 v/w)(VWR Chemicals, USA) under gentle stirring for 2 h. Granules were recovered by filtration using Whatman no 1 paper and a vacuum pump and dried overnight in an oven at 40 °C. Delipidated egg yolk granules were stored in a freezer at −20 °C until use. In order to determine the amount of protein and lipid contained in the delipidated egg yolk granules, they were previously dried overnight at 50 °C. Total nitrogen was analysed according to the Dumas method by using a CNHS/O elemental analyser (Vario El Analyzer, Elementar, Germany). Lipid content was analysed by using a Soxhlet-based device (Det-Gras 6 places, Selecta, Spain). Delipidated granules contained 92.5 ± 2.2 % proteins and 5.1 ± 1.5 % (w/w) lipids.

2.2. Preparation of nanoparticles and ultraviolet treatment

In order to prepare the nanoparticles, 1.5 g of delipidated egg yolk granules were mixed with 95 mL of deionized water (hereafter referred to as water) and 1.5 mL of 1 M NaOH. This solution was stirred at 65 °C for 20 min to obtain a homogeneous solution and then centrifuged at 10,000 r/min for 10 min (Heraeus Multifuge X1, Thermofisher, USA). The supernatant was recovered, and the concentration of solubilised protein was determined by the Lowry method and then adjusted to 2.5 mg/mL by diluting with distilled water. The pH of this solution was adjusted to different pH values from 10.0 to 7.0 and the particle size was measured. At pH 8.0, protein-based nanoparticles were spontaneously formed by self-assembly. In addition, the effect of ultraviolet light as a nanoparticle stabilising agent was also evaluated. For that purpose, 300 mL of the nanoparticle dispersion at pH 8.0 was introduced in a UV photochemical reactor and irradiated at different times with a medium pressure 150 Watt UV lamp (TQ 150, Heraeus Noblelight HmbH, Germany), operated by using a vertically orientated quartz immersion tube (30.5 cm length, 1.5 cm diameter) in the reaction liquid. The photochemical reactor was placed in an ice bath to keep suspensions from overheating and the nanoparticles solution was kept under gentle stirring during the experiment. After the UV-C treatment, the pH of the nanoparticle dispersion was adjusted to 7.0, since it is a more convenient pH for food-related applications, and then centrifuged at 13,000 r/min for 50 min. Afterwards, the supernatant was discarded and the amount of protein in the sediment was determined by Lowry's method. Finally, in order to characterise the nanoparticles produced, the nanoparticles in the sediment were dispersed in water at a concentration of 0.1 % (w of protein/v of water) using an ultrasound device (Sonopuls HD 2070, Bandelin, Germany) with a Titanium Microtip Probe (MS73 probe, Bandelin, Germany).

2.3. Nanoparticle characterisation

2.3.1. Particle size and zeta potential

The mean particle diameter, polydispersity index (PDI) and the zeta potential of the nanoparticles formed by self-assembly at pH 8.0 were measured at 25.0 °C using a dynamic light scattering (DLS) device (Zetasizer Nano ZS, Malvern Instruments, UK). In addition, after the ultraviolet treatment and the pH adjustment of the samples to 7.0, as described in section 2.2, the measurement was conducted using the same parameters as previously stated. To minimize the occurrence of multiple scattering effects, the nanoparticle dispersion was diluted with deionized water to achieve an appropriate concentration prior to measurement. Each sample was measured in triplicate to ensure reliable results (Rashidinejad, Birch, Sun-Waterhouse, & Everett, 2014).

2.3.2. Nanoparticle morphology

A drop of the nanoparticle solution was placed on a copper grid and negatively stained with a drop of uranyl acetate 1 % (w/v). The micrographs were obtained using a transmission electron microscope (TEM) (JEM-2000 EX-II, JEOL, Japan) operated at 100 kV.

2.3.3. Pattern of intra-particle interactive forcesn

The cohesive interactions within the nanoparticles were studied by measuring changes in their particle size when they were dispersed in different solvents (Liu & Tang, 2016). For that purpose, the nanoparticles were dispersed in distilled water, 1 % sodium dodecyl sulphate (SDS), 30 mM dithiothreitol (DTT), and 6 M urea. Afterwards, the dispersions were kept for at least 30 min under gentle stirring prior to determining the average size of the nanoparticles by DLS.

2.3.4. Nanoparticle wettability

Wettability measurements were carried out in order to study the hydrophobicity of the nanoparticles using the Washburn method (Alwadani, Ghavidel, & Fatehi, 2021). In this regard, the wettability of

the samples was measured with pure water and soybean oil with a tensiometer (Sigma 700, KSV Instruments Ltd., Finland).

For that purpose, nanoparticles were prepared and lyophilized. The solid powder, 0.25 g, was placed in a powder wettability measuring device (T112A, KSV Instruments Ltd., Finland) with a porous bottom and two screw threads in order to uniformly pack the sample. The porous bottom of the cylinder was brought into contact with water or oil and the liquid rose from the bottom and then through the sample, penetrating the powder by capillary force. All experiments were conducted at room temperature for 150 min, since preliminary measurements indicated that times longer than 100 min were required to obtain constant adsorbed mass values.

2.3.5. $ABTS^+$ free radical scavenging and ferrous chelating assays

The antioxidant activity of the nanoparticles was tested by $ABTS^+$ decolorization assay according to the method described by Khan, Fang, Cheng, Gao, Deng, and Liang (2019). For that purpose, a 7.0 mM $ABTS^+$ stock solution containing 2.5 mM potassium persulfate was prepared. This stock solution was maintained in darkness for 16 h and then diluted with water to obtain a working solution with an absorbance of 0.70 ± 0.04 measured at 734 nm in a spectrophotometer. Afterwards, 1 mL of the nanoparticle dispersion produced according to the methodology described in section 2.2 was mixed with 4 mL of the $ABTS^+$ working solution and kept in darkness for 20 min. Finally, the absorbance was measured at 734 nm. Regarding the ferrous ion chelating ability of the nanoparticles, this property was measured according to Sassi, Marcet, Rendueles, Díaz, and Fattouch (2020). Briefly, at the end of the preparation process the nanoparticles were recovered by centrifugation as stated in Section 2.2. The sediment was redispersed in the same volume of water containing $FeCl_2$ 2.0 mM and the dispersion was kept under gentle stirring for 5 min at room temperature. Afterwards, the dispersion was centrifuged at 15,000*g* for 50 min and the sediment was discarded. The supernatant was mixed with 0.2 mL of 5.0 mM ferrozine and after 5 min the absorbance of the solution was measured at 562 nm using a spectrophotometer (GENESYS™ 150 UV–Vis, Thermo Scientific, USA). The scavenging activity of the nanoparticles for both $ABTS^+$ and ferrous ion was calculated using the following equation:

$$Scavenging\ \ activity(\%) = \frac{A_c - A_t}{A_c} \times 100 \quad (1)$$

Where A_t is the absorbance of the nanoparticle sample at 734 nm for the $ABTS^+$ assay or at 562 nm for the ferrous ion chelating assay and A_c is the absorbance of the negative control that was prepared using water instead of the nanoparticle sample.

2.4. Pickering emulsion preparation

Nanoparticles were centrifuged and dispersed in distilled water at several concentrations (0.16–2.00 %, w/w) using an ultrasonic device. Emulsions were prepared with 25 % (w/w) of soybean oil (Sigma-Aldrich, USA) as oil phase and the nanoparticles suspension as aqueous phase. This relatively low percentage of dispersed phase volume fraction was selected in order to accelerate destabilization processes such as creaming.

Emulsions were prepared by mechanical agitation at 15,000 r/min for 2 min using a homogeniser (Silent Crusher M, Heidolph, Germany).

2.5. Emulsion characterisation

2.5.1. Emulsion average droplet size

The particle size distributions of the prepared Pickering emulsions were measured with a static light scattering device (Mastersizer S, Malvern Instruments Ltd., UK) according to the methodology employed by Östbring, Matos, Marefati, Ahlström, and Gutiérrez (2021). In this case, a level of obscuration between 10 and 20 % was achieved before each measurement and a refractive index (RI) value of 1.456 and 1.33 was used for soybean oil and water, respectively. In addition, the pump velocity was adjusted to 1600 r/min.

2.5.2. Optical microscopy

In order to visualize the emulsion droplets, microscopy images were obtained using an optical microscope (Leica DM E, Leica, USA). For that purpose, a volume of 10 μL of the emulsion was placed onto a glass slide and covered with a square cover glass. Images were captured with a CCD camera connected to the microscope using a 20× magnification level.

2.5.3. Rheology

Rheological tests were performed with a rotational rheometer (Haake MARS II, Thermo Fisher Scientific, USA) using a PP60ti probe and a Peltier unit to control the temperature. The sample was placed between the plate/plate measuring system with a gap of 1 mm, any excess of sample was removed before testing. All the samples were allowed to rest for 15 min before any measurement to relax the stress and stabilize the temperature (20 ± 0.1 °C). In steady state, the apparent viscosity of the emulsions was obtained as a function of shear rate from 0.01 1/s to 500 1/s in 500 s. In dynamic conditions, frequency-dependence tests were performed from 10.00 Hz to 0.01 Hz at a constant shear stress of 1 Pa. The experimental data obtained were adjusted to the following power law equation according to Gabriele, de Cindio, and D'Antona (2001).

$$G^* = A \times \omega^{1/z} \quad (2)$$

Where G^* is the complex modulus in Pa. The complex modulus is a measure of the overall resistance of the emulsion to deformation, ω the frequency in Hz, Z (dimensionless) the coordination number and A the proportional coefficient (Pa).

2.5.4. Emulsion storage stability

The Pickering emulsions storage stability was assessed with a Static Multiple Light Scattering (SMLS) equipment (Turbiscan Lab Expert, Formulaction, France), according to Rezvani et al. (2022). For that purpose, undiluted samples were placed in test cells and the back-scattered light was monitored at several times for 80 days at 30 °C using an automated ageing station (Turbiscan AGS, Formulaction, France). Samples were scanned by the optical reading head and the Transmission (TS) and Backscattering (BS) data were obtained every 40 μm as a function of sample height (in mm). After the measurement performed at each time, a macroscopic fingerprint of the emulsion was obtained, providing information about the appearance of a clarification layer, the creaming processes, and the droplet size distribution. In addition, the Turbiscan Stability Index (TSI) was also calculated in order to obtain a key value for the general behaviour of the tested emulsions, allowing comparison between different formulations. This parameter was calculated according to the following eq. (Luo et al., 2017):

$$TSI = \sum_i \frac{\sum_h |scan_i(h) - scan_{i-1}(h)|}{\mathrm{H}} \quad (3)$$

Where H is the total height of the cell and $scan_i(h)$ is the backscattering value resulting from the scanning of the sample at a given time and height.

2.6. Statistical analysis

Experiments were performed in triplicate and are shown as the mean value ± standard deviation of three independent experiments (n = 3). Least significant differences (LSD) were calculated by Fisher's test with a level of significance of $P < 0.05$ to determine significant differences between the tested samples. These analyses were performed using Statgraphics® V.15.2.06 statistical software.

3. Results and discussion

3.1. Nanoparticles preparation

Delipidated proteins from egg yolk granules were obtained and solubilised at pH 11.0, since at such a high pH the net charge of proteins is strongly negative, which keeps them dissolved in the aqueous solution as a result of repulsive electrostatic forces. However, as the pH of the solution decreases and approaches the isoelectric point of the proteins, a certain degree of aggregation occurs because the overall net charge becomes closer to zero (T. Zhang et al., 2021). Egg yolk granules are mainly comprised of two proteins, the high-density lipoproteins (HDL), which represent 70 % of the granules' dry matter, and the phosvitin, which constitutes 16 % (I Marcet et al., 2022). Focussing on the principle component, the solubility of HDL in distilled water is close to 100 % at pH 10.0 but shows a sharp decrease at pH 8.0 and below, with a solubility lower than 10 % at pH 7.0–8.0, while the HDL becomes almost completely insoluble in the pH range from 5.0 to 6.0 (Chalamaiah, Esparza, Hong, Temelli, & Wu, 2018). In this regard, according to the results shown in Fig. 1A, the previously dissolved granular proteins formed aggregates of 45.6 ± 1.4 nm at pH 8.0, but a decrease in the pH to 7.0 led to a decrease in the negative zeta potential value of the nanoparticles and thus an increase in their size to 431.8 ± 75.7 nm. Therefore, it must be underlined that this average size value at pH 7.0 is 970 % higher than that found for the same nanoparticles at pH 8.0. For this reason, nanoparticles were primarily prepared at pH 8.0 by self-assembling.

Usually, nanoparticles stabilised by covalent bonds have higher structural stability and are less sensitive to environmental changes. In this case, UV radiation has been tested in order to improve the pH stability of the prepared nanoparticles. For this purpose, nanoparticles formed at pH 8.0 were irradiated with UV-C in order to stabilise them, and then the pH of the suspension was lowered to pH 7.0, which is a more convenient pH for food-related applications. The effect of this treatment on the average size and Z potential is shown in Fig. 1A, and the PDI is shown in Table S1. According to the results obtained, nanoparticles had a size of 44.9 ± 1.1 nm after 10 min of UV-C treatment at pH 8.0, but a subsequent decrease of the pH of the dispersion to 7.0 produced an increase in the nanoparticle size to 139.7 ± 5.9 nm, which represents an increase in size of 311 %, much lower than the 970 % measured for the untreated nanoparticles. In addition, the zeta potential was not affected by the UV-C treatment, a value of −15.10 mV being measured for the nanoparticles irradiated for 10 min. Although values for this parameter in the range from +20 to −20 mV are indicative of instability because the repulsive forces are not strong enough to avoid the aggregation of the particles (Sow, Chong, Liao, & Yang, 2018), in this case, after 10 days of storage at 4 °C, the size of these nanoparticles irradiated for 10 min remained unchanged (130.4 ± 10.2 nm; $P < 0.05$). The molecular changes underlying the stabilising effect of the UV-C treatment can be attributed to the absorption of UV radiation by the

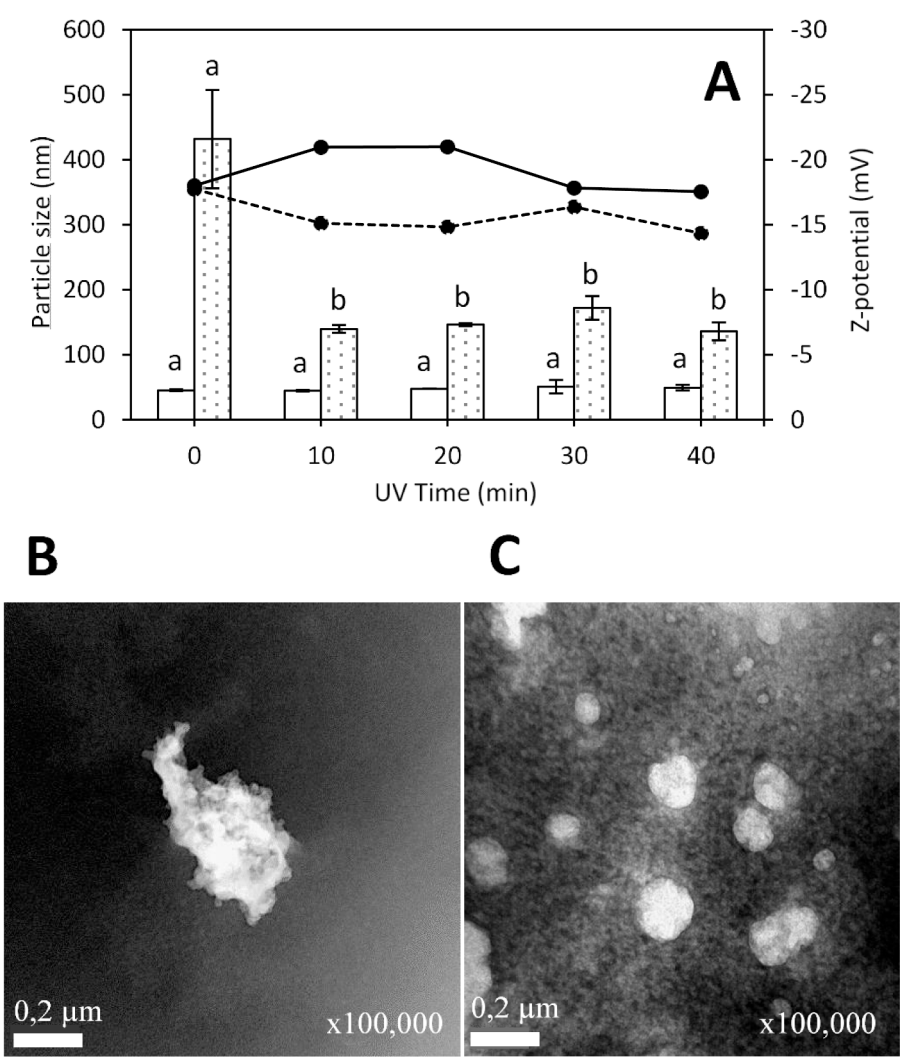

Fig. 1. Zeta average (white bars: pH 8 particles; dotted bars: pH 7 particles) and zeta potential values (continuous line: pH 8 particles; dashed line: pH 7 particles) of the egg yolk protein-based nanoparticles exposed for several different time periods of UV-C radiation at pH 8.0 and 7.0 (**A**); TEM micrographs of the egg yolk protein-based nanoparticles at pH 7.0 without UV treatment (**B**) and treated for 10 min with UV-C (**C**). Different superscript letters in the columns of different pH indicate significant differences ($P < 0.05$).

aromatic rings present in the amino acids of the egg yolk proteins. This absorption leads to the generation of free radicals, which subsequently initiate the formation of intramolecular covalent bonds (de Vargas, Marczak, Flôres, & Mercali, 2022). These covalent bonds could be fixing the spatial conformation of the nanoparticles, thus hindering the movement of the proteins and preventing their aggregation to some extent. According to the results obtained, more than 10 min of UV-C exposition did not produce any improvement in the stability of the nanoparticles, so the following tests were performed only on nanoparticles treated for 10 min with UV-C radiation at pH 8.0 followed by a pH adjustment to 7.0, since this pH is more usual in food products than pH 8.0 (Andrés-Bello, Barreto-Palacios, García-Segovia, Mir-Bel, & Martínez-Monzó, 2013).

3.2. Nanoparticle morphology

TEM micrographs of the prepared nanoparticles are shown in Fig. 1B, C. As can be observed, the UV-C-treated nanoparticles had a spherical-like morphology and an average diameter similar to that measured by DLS. These treated nanoparticles also showed a less than completely smooth surface, which is a usual characteristic of protein-based nanoparticles that has been frequently reported by other authors (Zhao, Shen, Zhang, Zhong, Zhao, & Zhou, 2021). By contrast, particles without UV-C treatment at pH 7.0 (Fig. 1B) showed a completely irregular shape and greater size when compared with the treated ones.

3.3. Intra-particle interactive forces

The intra-particle interactive forces established within the nanoparticles treated with UV-C for 10 min and those of the untreated ones were evaluated by dispersing these nanoparticles in SDS, DTT and urea, and then measuring changes in their average size in relation to their size in water. In this regard, SDS is able to disrupt hydrophobic interactions, DTT disulphide bonds and urea hydrogen bonds. According to the results shown in Fig. 2, untreated nanoparticles were markedly affected and to the same extent by both SDS and urea, which is usual for this type of nanoparticle, since protein aggregation is mainly driven by non-covalent bonds (Ren et al., 2021). In addition, the presence of DTT in the medium also affected the average size of the nanoparticles, but in this case the aggregates formed were of larger size. This behaviour was also observed by other authors working with soy-glycinin nanoparticles (Liu et al., 2016) and although the underlying mechanism is not completely understood, it may be due to the rupture of the disulphide bonds producing unfolding of the proteins and the exposure of more hydrophobic regions, which may enhance protein aggregation and increase the size of the nanoparticles. On the other hand, UV-treated nanoparticles showed a low sensitivity to the chemicals used in this assay. In fact, although the urea and SDS produced an increase in the average size of the nanoparticles, no statistically significant difference was observed compared with the nanoparticles dispersed only in water ($P < 0.05$). A similar result was obtained when the nanoparticles were dispersed in the DTT solution. As was mentioned, UV radiation is absorbed by protein double bonds and aromatic rings causing the formation of radical groups and the subsequent formation of new inter- and intra-molecular covalent bonds. These new covalent bonds were insensitive to the chemicals used in this experiment and seemed to fix the internal structure of the nanoparticles, limiting the disruptive effect of the SDS, urea and DTT on the nanoparticle size.

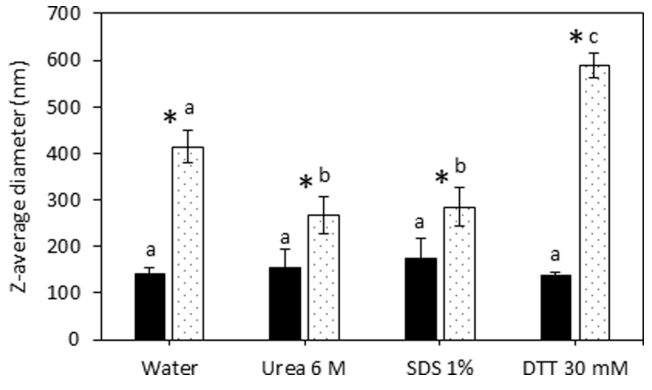

Fig. 2. Effect of Urea, SDS and DTT on the Z-average diameter of the egg yolk protein-based nanoparticles irradiated with UV-C for 10 min (black bars) and non-irradiated (white dotted bars) at pH 7.0. Asterisk indicates significant differences between irradiated and non-irradiated samples, and different superscript letters in the same column indicate significant differences ($P < 0.05$).

3.4. Nanoparticle wettability

From Fig. 3 it can be observed that soybean oil was absorbed into the pressed nanoparticle sample within a few seconds and the maximum weight of oil adsorbed by 0.25 g of nanoparticles remained constant at 0.42 g during the test period. However, in the case of wettability with water, the adsorption was more gradual and a constant weight value was not registered until one hour, when the maximum adsorption corresponded to 56.0 g of water per 0.25 g of nanoparticles used. Therefore, according to these results, nanoparticles have a clearly intermediate wettability for oil and water, their wettability being greater in water, which makes this type of particle suitable for the preparation of stable oil in water emulsions.

3.5. ABTS + free radical scavenging and ferrous chelating assays

Egg yolk granules showed antioxidant properties when they were used to stabilise algal oil (Li et al., 2021) or to encapsulate polyphenols (Sassi et al., 2020). Most of the antioxidant properties of egg yolk granules have been related to the presence of phosvitin, the most highly phosphorylated protein found in nature, whose antioxidant and chelating properties and those of its hydrolysates have been studied by many authors (I Marcet et al., 2022). The nanoparticles prepared in this study and treated for 10 min with UV-C showed high ABTS cation radical scavenging activity (53.23 ± 0.19 %) and ferrous ion chelating properties (82.33 ± 1.20 %), as might be expected, given that 16 % of the protein content of the granular fraction is phosvitin. Similar ferrous ion chelating properties were described by other authors working with extracted phosvitin (Jung, Jo, Kang, Ahn, & Nam, 2012).

3.6. Pickering emulsions

In order to prepare Pickering emulsions, only the nanoparticles treated with UV-C radiation for 10 min were considered. As was commented previously, these nanoparticles were significantly smaller and

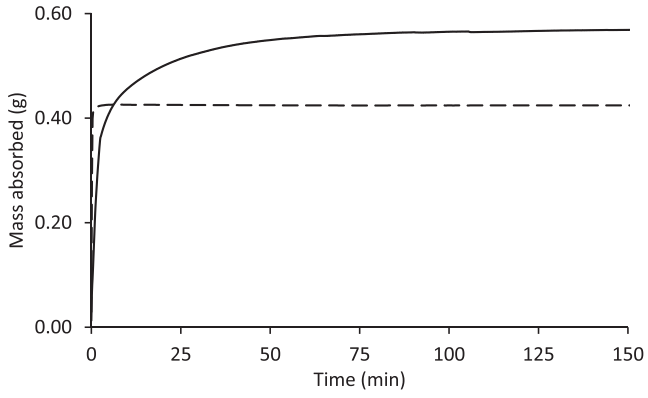

Fig. 3. Wettability in soybean oil (dashed line) and water (continuous line) of the egg yolk protein-based nanoparticles treated with UV-C for 10 min.

more stable at pH 7.0 than the untreated nanoparticles.

3.6.1. Effect of the protein concentration on the drop size distribution of the Pickering emulsions

The influence of the nanoparticle concentration on the fundamental properties of the prepared Pickering emulsions is shown in Fig. 4. Droplet size distribution and mean average diameter values ($D_{(4,3)}$) of fresh prepared emulsions using nanoparticles as stabilizer are shown in Fig. 4A,C. Additional diameter values ($D_{(3,2)}$, $D_{(v,0.5)}$ and span) can be found in Table S2. Considering all tested nanoparticle concentrations, the lowest $D_{(4,3)}$ value measured was 29.09 μm for the 1 % nanoparticle concentration formulation, and the highest $D_{(4,3)}$ value measured was 77.15 μm for the 0.16 % sample. These mean average diameter values are similar to others found in the literature for Pickering emulsions prepared with protein-based nanoparticles (Xiao et al., 2016).

Furthermore, all tested emulsions presented a unimodal particle size distribution showing a large reduction in droplet size when the concentration of nanoparticles went from 0.16 up to 1 %. The use of a nanoparticle concentration greater than 1 % resulted in emulsions with a wider size distribution and with a slight increase in the average droplet size. No differences were observed when the nanoparticle concentration was increased from 1.33 to 2 % ($P < 0.05$), although a decrease in the oil droplet size might have been expected as the concentration of stabilizer, in this case protein nanoparticles, increased. However, it must also be considered that this effect of the stabilizer concentration on the droplet size must necessarily have a limit, which is usually related to the size of the particles acting as Pickering emulsifier and the emulsification method. Therefore, once that saturation point is reached, the excess of particles will be found in the continuous phase (Tcholakova, Denkov, Sidzhakova, Ivanov, & Campbell, 2003).

In this regard, the theoretical number of nanoparticles necessary to fully cover the oil droplets was calculated according to the experimental mean surface diameter values obtained ($D_{(3,2)}$), available in Table S2. The specific surface area (S) of an emulsion is by definition:

$$S = \frac{6\phi}{D_{(3,2)}} \tag{4}$$

Full coverage calculations were performed according to Matos, Laca, Rea, Iglesias, Rayner, and Gutiérrez (2018), assuming that nanoparticles have a spherical shape and that they are packed together at the oil droplet surface. Equation (5) allows the calculation of the full surface coverage as mass of particles per mass of oil ($\Gamma_{p/o}$):

$$\Gamma_{p/o} \frac{N_{p/d} V_p \rho_p}{V_d \rho_{oil}} \tag{5}$$

Where $N_{p/d}$ is the number of particles to cover an oil drop, V_p and V_d are the volume of a particle and the oil drop respectively, ρ_p is the density of the protein nanoparticles, which was assumed to be the same as the density of proteins (1.35 kg/L) and ρ_{oil} is the density of the oil used (0.995 kg/L).

While $N_{p/d}$ was calculated by the following equation:

$$N_{p/d} = \frac{A_d}{A_{tp}} \tag{6}$$

Where A_d and A_{tp} are the area of a drop and the transversal area of a protein nanoparticle.

According to the results shown in Fig. 4D, it can be observed that when the 0.16 and 0.33 % nanoparticle concentrations were tested, the theoretical calculated coverage was larger than the experimental value that was used, which could indicate that these emulsions could easily have irreversible destabilization due to coalescence or to the promotion of Ostwald ripening behaviour (Matos, Marefati, Barrero, Rayner, & Gutiérrez, 2021). In fact, after 10 days of storage (Fig. 4B,C), a slight increase in the $D_{(4,3)}$ value for the 0.16, and 0.33 % samples was observed, which may be produced due to coalescence. However, a much

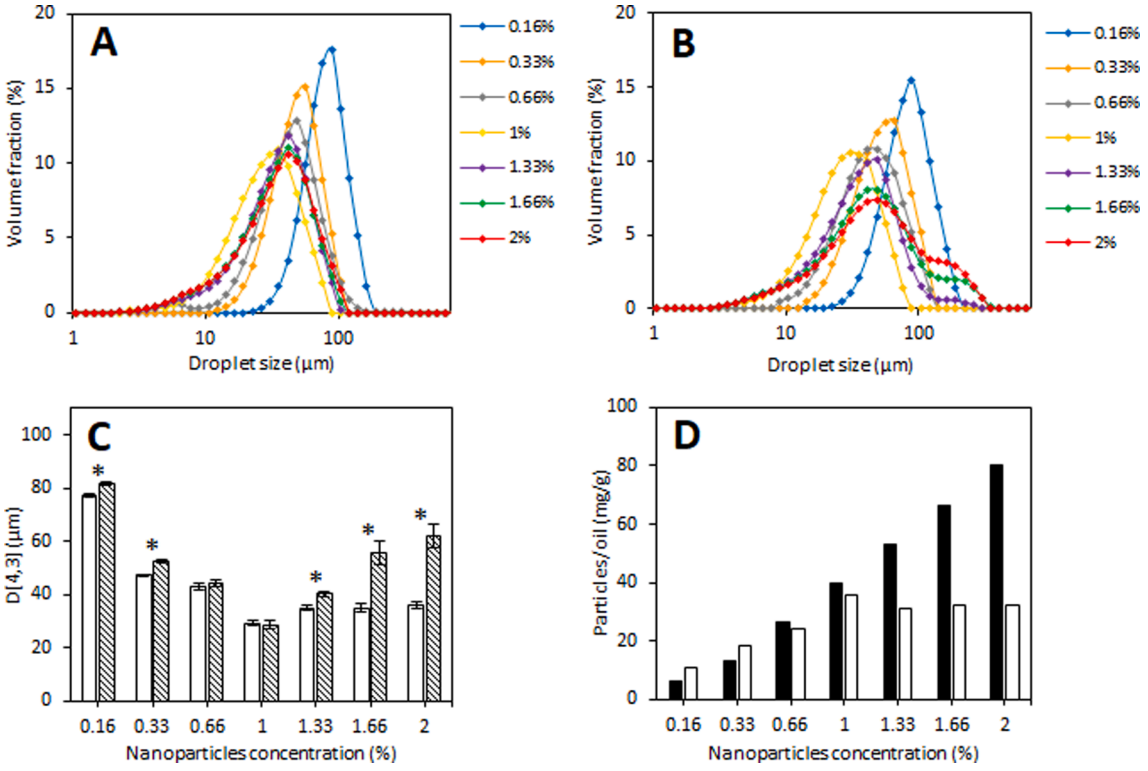

Fig. 4. Effect of the nanoparticle concentration on the properties of the Pickering emulsions. Droplet size distribution of fresh prepared emulsions (**A**) and after 10 days of storage (**B**); mean average diameter ($D_{(4,3)}$) of fresh emulsions (white bars) and emulsions stored for 10 days (dashed bars), asterisk indicate significant differences ($P < 0.05$) between fesh and stored emulsions (**C**); and theoretical (white bars) and experimental (black bars) nanoparticle concentrations required for the full coverage of the oil droplets (**D**).

higher increase in this $D_{(4,3)}$ value was recorded for the 1.66 and 2 % samples after 10 days of storage, in part due to the appearance of a large fraction of oil droplets that cannot be explained by a deficiency in the nanoparticle coverage of the oil surface. In this case, the measured increase in the droplet size may occur due to the high presence of nanoparticles in the continuous phase, which enhanced the interaction between them and between them and the nanoparticles located on the surface of the oil droplets, leading to an aggregation and/or coalescence phenomenon.

The optical microscopy images of the fresh emulsions are shown in Figure S1, and they were found to be consistent with the results of the droplet size distribution and mean average diameter value discussed previously. The observed oil droplets decreased in size as the nanoparticle concentration was increased until reaching a concentration of 1 %, no additional decrease in the oil droplet size being observed in the nanoparticle concentration range between 1 % and 2 %.

3.6.2. *Rheological behaviour*

The fluid behaviour of the Pickering emulsions is shown in Fig. 5A. As can be observed, the apparent viscosity of all tested samples decreased with increasing shear rate, which is a characteristic of shear-thinning fluids. This phenomenon may be primarily attributed to the progressive disruption of the interparticle forces produced between the nanoparticles adsorbed at the surface of different oil droplets, these forces being more difficult to reassemble as the shear rate increases. Furthermore, the apparent viscosity of the emulsions was higher with increasing nanoparticle concentration in the 0.16–1 % range. The emulsions prepared within this range of nanoparticle concentrations showed a progressive decrease in the oil droplet size, which resulted in an increasing number of oil droplets that were able to establish a higher number of interactions between them, producing more packed emulsions with a higher viscosity. This effect of the concentration of stabilizer on the apparent viscosity of Pickering emulsions has been similarly described by other authors working with nanoparticles prepared with gelatine and tea proteins (Feng et al., 2020; Ren et al., 2021). However, this tendency changed from the 1.33 % to the 2 % samples, a progressive decrease in the viscosity of the emulsions appearing as the nanoparticle concentration increased.

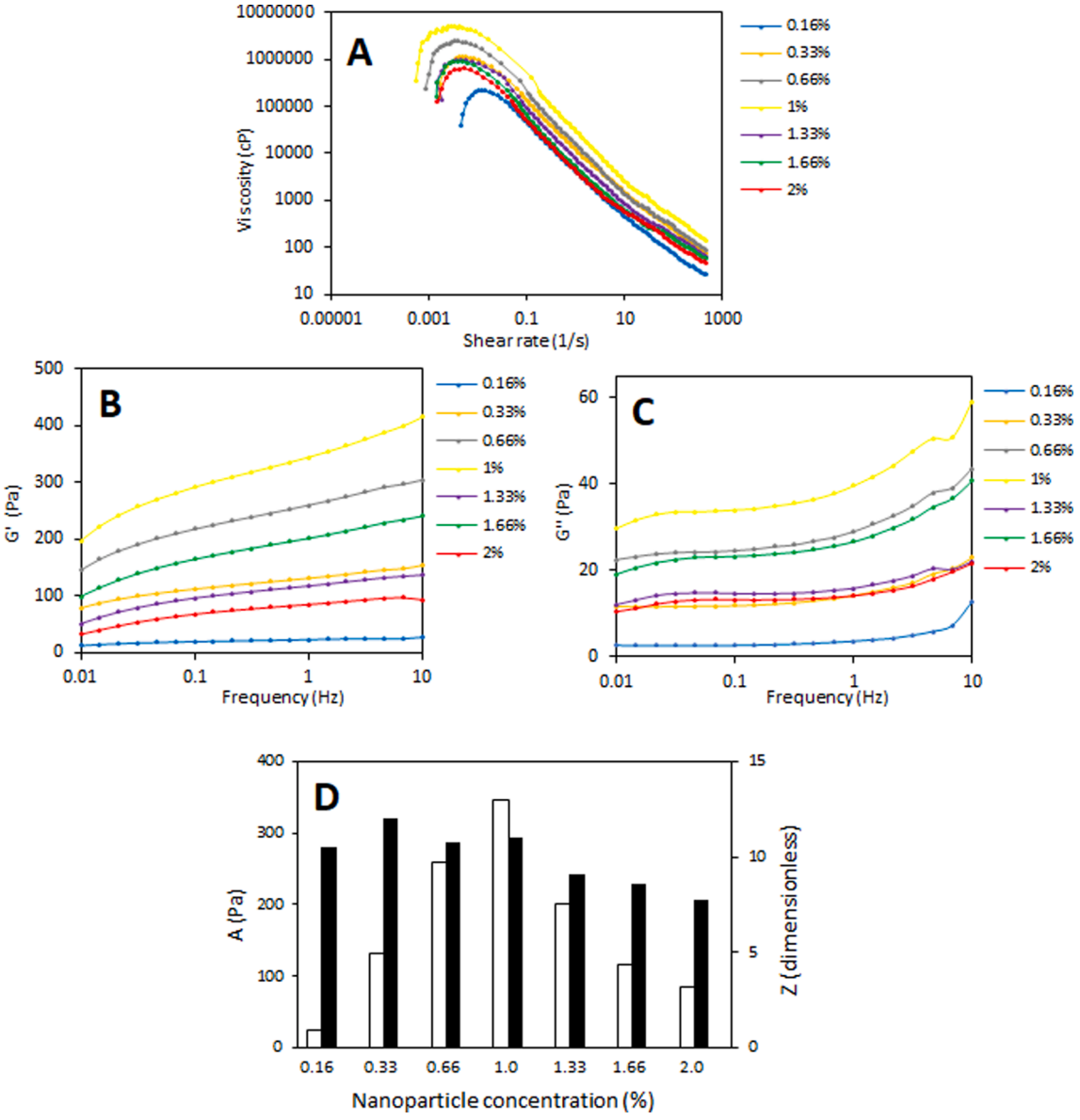

Fig. 5. Plots of the apparent viscosity (**A**) and mechanical spectra (**B**, G′; **C**, G″) of the Pickering emulsions prepared with different protein nanoparticle concentrations; coordination number (*Z*, black bars) and proportional coefficient (*A*, white bars) calculated from the frequency sweeps presented in 5B and 5C (**D**).

A similar trend was detected when the frequency sweeps were conducted. According to the results shown in Fig. 5B,C, all samples showed a higher G′ than G″ value over all the frequency range and a noticeable frequency dependence of both moduli within the range studied, all this suggesting that the samples were structured in the form of a soft-gel (Ismael Marcet, Paredes, & Díaz, 2015). In addition, the increase in the G′ and G″ values with the increase of the nanoparticle concentration over the range of 0.16–1 % denotes samples with a higher degree of structuring, likely due to the incorporation of more nanoparticles to the oil–water interface, but this trend was reversed within the nanoparticle concentration range of 1.33–2 %, a decrease in the value of both moduli being observed as the concentration of nanoparticles was increased. Therefore, although the emulsions prepared in this range of concentrations resulted in fresh emulsions with a droplet size similar to the 1 % preparation, they not only showed a higher instability after 10 days of storage (Fig. 4C), but also when subjected to mechanical stress.

Furthermore, the complex modulus was obtained from the mechanical spectra of each emulsion and the coordination number (*Z*) and the proportional coefficient (*A*) were calculated according to the power law equation presented in section 2.5.3. Values obtained are shown in Fig. 5D.

The dimensionless parameter *Z* is related to the number of rheological units in the network, while the *A* (Pa) parameter shows the strength of the interaction between those units (Gabriele et al., 2001). According to these results, higher A values were obtained as nanoparticle concentration increased from 0.16 to 1 %, which is related to the formation of stronger networks within the emulsions. However, further increases in concentration produced the opposite effect, weakening the network. Furthermore, the *Z* parameter showed similar behaviour and the highest values were obtained in the nanoparticle concentration range from 0.16 to 1 %, but it progressively decreased from the 1.33 to the 2 % concentration. Bearing in mind that higher *Z* and *A* values are related to more stable emulsions (Heydari & Razavi, 2021), these results confirm the destabilizing effect of the nanoparticles at the highest concentrations tested in this study.

A high nanoparticle concentration increases the aqueous phase thickness, enhancing entropic and steric repulsions, which prevents the movement and coalescence of droplets. However, in this case, an optimum value was detected, above which the use of larger protein concentrations resulted in larger oil droplet sizes in fresh emulsions and in lower emulsion stability after 10 days of storage (Fig. 4C). This destabilising effect may exist because, at such high nanoparticle concentrations, interactions started to be established between the particles, forming a flocculated network, while interactions also taking place with nanoparticles located at the oil/water interface promoted the aggregation of the oil drops. This increase in the droplet size led to the lower apparent viscosity and lower G′ and G″ values shown in the rheology testing.

A similar kind of behaviour was observed by Ahlström et al. (2022), who studied the emulsifying properties of rapeseed proteins. According to their findings, the oil droplet size was slightly increased at the highest concentrations of protein tested when it was extracted at pH 5.0, 5.5 and 6.0, also producing emulsions that were less stable under storage conditions.

3.6.3. Stability

After 80 days of storage at 30 °C, it was observed that all samples presented a clarification or serum layer at the bottom of the test sample due to the lower density of the oil droplets compared to the density of the aqueous phase, which involved the migration of the droplets to the surface. Most of this oil-droplet migration phenomenon happened during the first 24 h of storage, which is usual behaviour for these emulsions (Matos et al., 2021). Fig. 6A summarizes the relative size of the clarification or serum layer, emulsion and oil layers found after 80 days of storage in the test cells for every sample tested, observing that the creaming process exhibited nanoparticle concentration dependent behaviour, and hence the emulsions prepared with a higher concentration of nanoparticles presented a thin clarification layer. However, looking at the part of the emulsion layer, it was seen that additional destabilization phenomena, including coalescence or Ostwald ripening, were present for those emulsions prepared with the highest nanoparticle concentrations tested. In this regard, the global TSI values during the test time, which were obtained considering both the clarification and the emulsion layers, are shown in Fig. 6B, bearing in mind that lower TSI values during emulsion ageing implies a higher stability (Boostani, Riazi, Marefati, Rayner, & Hosseini, 2022). These TSI values confirmed

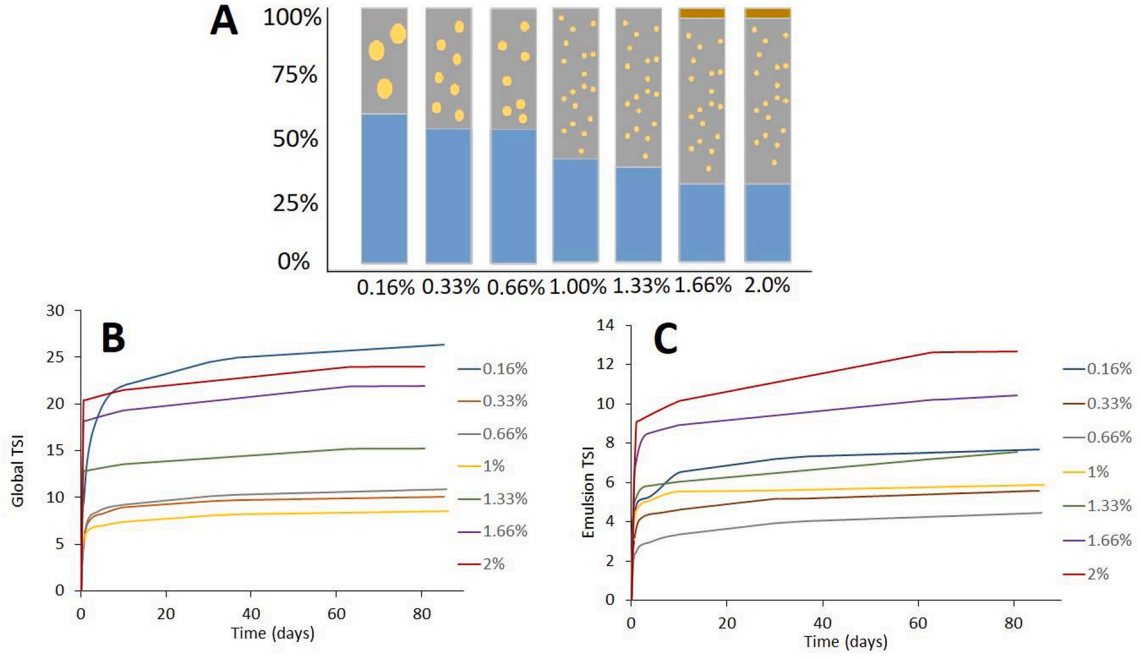

Fig. 6. Relative size of the clarification layer, emulsion and oil layers found after 80 days of storage in the Turbiscan test cells for each emulsion tested (**A**). Global (**B**) and emulsion (**C**) TSI values over 80 days of storage for the same Pickering emulsions.

that the 1 % sample was the most stable, with a TSI value of 8.5 after 80 days of storage, closely followed by the 0.33 and 0.66 % samples, with a TSI value of 10.1 and 10.8, respectively. It should be underlined that these three emulsions showed the most similar theoretical and experimental particles/oil coverage values among all samples tested. In addition, it was also found that the emulsion prepared with 0.16 % of nanoparticles presented the largest TSI value due to its large clarification layer, which in turn is related to the bigger size of the oil droplets found in this sample (Fig. 4). The following most unstable emulsions were those prepared with 1.66 and 2 % nanoparticle concentrations, which confirms their destabilizing effect at the highest concentrations tested. In this sense, according to Stokes law, it has to be considered that the viscosity of an emulsion is closely related to its stability, since the oil droplets in a low viscosity medium tend to suffer more easily from flocculation and coalescence (Yue, Huang, Zhu, Huang, & Huang, 2022), being precisely the 0.16 %, 1.66 % and 2 % samples those with the lowest apparent viscosity (Fig. 5A).

Furthermore, in order to evaluate only the effect of the coalescence on the stability of the emulsions, the TSI parameter was calculated once more but without including the clarification layer found at the bottom of the test cell (Fig. 6C). In this case, the TSI values presented a different trend, since the emulsions prepared with 0.16 % of nanoparticles showed an intermediate stability, the emulsions with the largest nanoparticle concentrations, those prepared with a concentration of 1.66 and 2 %, being the ones with the highest instability.

And once again, the emulsions with the highest stability correspond to the 0.33, 0.66 and 1 % samples. These results are in accordance with the results of rheological properties and droplet size measurement, suggesting that there is an optimal concentration of nanoparticles that produces a high stabilization of the emulsion, but once this concentration is exceeded, the excess of nanoparticles enhances the coalescence of the oil droplets and significantly decreases the stability of the emulsion.

4. Conclusions

The new nanoparticles prepared from delipidated egg yolk granular proteins and stabilised with UV-C that were developed in this study showed an adequate size, morphology and wettability for use as Pickering emulsifiers. In addition, these nanoparticles had antioxidant and ferrous ion chelating properties, which could make them useful not only to prepare emulsions, but even to prevent the oxidation of other types of foodstuffs. These bioactivities increase their value as an ingredient for the food industry. Furthermore, encapsulating bioactive compounds using these novel nanoparticles is a feasible possibility that was not covered in this work. Regarding the Pickering emulsions prepared with these nanoparticles, the present study demonstrated that the emulsions prepared with UV-treated delipidated egg yolk granular proteins were highly stable, in particular those formulated with a 1 % nanoparticle concentration, and hence they are useful to significantly expand the range of applications of the egg yolk granular fraction in the food industry. In addition, UV-C was demonstrated to be a useful stabilising agent for these protein-based nanoparticles, which may be combined with other enzymatic or chemical crosslinking agents to further improve their stability.

CRediT authorship contribution statement

Florencia Ridella: Methodology, Formal analysis, Investigation, Writing – review & editing. **Ismael Marcet:** Conceptualization, Methodology, Formal analysis, Writing – review & editing. **Gemma Gutiérrez:** Methodology, Writing – review & editing. **Manuel Rendueles:** Supervision, Funding acquisition. **Mario Díaz:** Supervision, Funding acquisition.

Declaration of Competing Interest

The authors declare that they have no known competing financial interests or personal relationships that could have appeared to influence the work reported in this paper.

Data availability

Data will be made available on request.

Acknowledgements

This work was financially supported by the Scientific and Technical Research Foundation (FICYT) of the Principality of Asturias, by the project SV-PA-21-AYUD/2021/51041.

Appendix A. Supplementary material

Supplementary data to this article can be found online at https://doi.org/10.1016/j.foodchem.2023.137330.

References

Ahlström, C., Thuvander, J., Rayner, M., Matos, M., Gutiérrez, G., & Östbring, K. (2022). The Effect of Precipitation pH on Protein Recovery Yield and Emulsifying Properties in the Extraction of Protein from Cold-Pressed Rapeseed Press Cake. *Molecules, 27*(9), 2957.

Alwadani, N., Ghavidel, N., & Fatehi, P. (2021). Surface and interface characteristics of hydrophobic lignin derivatives in solvents and films. *Colloids and Surfaces A: Physicochemical and Engineering Aspects, 609*, Article 125656.

Andrés-Bello, A., Barreto-Palacios, V., García-Segovia, P., Mir-Bel, J., & Martínez-Monzó, J. (2013). Effect of pH on color and texture of food products. *Food Engineering Reviews, 5*(3), 158–170.

Boostani, S., Riazi, M., Marefati, A., Rayner, M., & Hosseini, S. M. H. (2022). Development and characterization of medium and high internal phase novel multiple Pickering emulsions stabilized by hordein nanoparticles. *Food Chemistry, 372*, Article 131354.

Chalamaiah, M., Esparza, Y., Hong, H., Temelli, F., & Wu, J. (2018). Physicochemical and functional properties of leftover egg yolk granules after phosvitin extraction. *Food Chemistry, 268*, 369–377.

de Vargas, V. H., Marczak, L. D. F., Flôres, S. H., & Mercali, G. D. (2022). Advanced Technologies Applied to Enhance Properties and Structure of Films and Coatings: A Review. *Food and Bioprocess Technology*, 1–24.

Díaz, O., Candia, D., & Cobos, Á. (2016). Effects of ultraviolet radiation on properties of films from whey protein concentrate treated before or after film formation. *Food Hydrocolloids, 55*, 189–199.

Fathi, N., Almasi, H., & Pirouzifard, M. K. (2018). Effect of ultraviolet radiation on morphological and physicochemical properties of sesame protein isolate based edible films. *Food Hydrocolloids, 85*, 136–143.

Feng, X., Dai, H., Ma, L., Fu, Y., Yu, Y., Zhou, H., … Zhang, Y. (2020). Properties of Pickering emulsion stabilized by food-grade gelatin nanoparticles: Influence of the nanoparticles concentration. *Colloids and Surfaces B: Biointerfaces, 196*, Article 111294.

Gabriele, D., de Cindio, B., & D'Antona, P. (2001). A weak gel model for foods. *Rheologica Acta, 40*(2), 120–127.

Heydari, A., & Razavi, S. M. A. (2021). Evaluating high pressure-treated corn and waxy corn starches as novel fat replacers in model low-fat O/W emulsions: A physical and rheological study. *International Journal of Biological Macromolecules, 184*, 393–404.

Jung, S., Jo, C.-R., Kang, M.-G., Ahn, D.-U., & Nam, K.-C. (2012). Elucidation of antioxidant activity of phosvitin extracted from egg yolk using ground meat. *Food Science of Animal Resources, 32*(2), 162–167.

Khan, M. A., Fang, Z., Cheng, H., Gao, Y., Deng, Z., & Liang, L. (2019). Encapsulation and protection of resveratrol in kafirin and milk protein nanoparticles. *International Journal of Food Science & Technology, 54*(11), 2998–3007.

Kiosseoglou, V., & Paraskevopoulou, A. (2005). Molecular interactions in gels prepared with egg yolk and its fractions. *Food Hydrocolloids, 19*(3), 527–532.

Li, J., Shen, Y., Zhai, J., Su, Y., Gu, L., Chang, C., & Yang, Y. (2021). Enhancing the oxidative stability of algal oil powders stabilized by egg yolk granules/lecithin composites. *Food Chemistry, 345*, Article 128782.

Lin, J., Meng, H., Yu, S., Wang, Z., Ai, C., Zhang, T., & Guo, X. (2021). Genipin-crosslinked sugar beet pectin-bovine serum albumin nanoparticles as novel pickering stabilizer. *Food Hydrocolloids, 112*, Article 106306.

Liu, F., & Tang, C.-H. (2016). Soy glycinin as food-grade Pickering stabilizers: Part. I. Structural characteristics, emulsifying properties and adsorption/arrangement at interface. *Food Hydrocolloids, 60*, 606–619.

Luo, M., Qi, X., Ren, T., Huang, Y., Keller, A. A., Wang, H., … Li, F. (2017). Heteroaggregation of CeO2 and TiO2 engineered nanoparticles in the aqueous phase: Application of turbiscan stability index and fluorescence excitation-emission

matrix (EEM) spectra. *Colloids and Surfaces A: Physicochemical and Engineering Aspects, 533*, 9–19.
Marcet, I., Paredes, B., & Díaz, M. (2015). Egg yolk granules as low-cholesterol replacer of whole egg yolk in the preparation of gluten-free muffins. *LWT-Food Science and Technology, 62*(1), 613–619.
Marcet, I., Sáez-Orviz, S., Rendueles, M., & Díaz, M. (2022). Egg yolk granules and phosvitin. Recent advances in food technology and applications. *LWT, 153*, Article 112442.
Matos, M., Laca, A., Rea, F., Iglesias, O., Rayner, M., & Gutiérrez, G. (2018). O/W emulsions stabilized by OSA-modified starch granules versus non-ionic surfactant: Stability, rheological behaviour and resveratrol encapsulation. *Journal of Food Engineering, 222*, 207–217.
Matos, M., Marefati, A., Barrero, P., Rayner, M., & Gutiérrez, G. (2021). Resveratrol loaded Pickering emulsions stabilized by OSA modified rice starch granules. *Food Research International, 139*, Article 109837.
Ning, F., Ge, Z., Qiu, L., Wang, X., Luo, L., Xiong, H., & Huang, Q. (2020). Double-induced se-enriched peanut protein nanoparticles preparation, characterization and stabilized food-grade pickering emulsions. *Food Hydrocolloids, 99*, Article 105308.
Östbring, K., Matos, M., Marefati, A., Ahlström, C., & Gutiérrez, G. (2021). The effect of ph and storage temperature on the stability of emulsions stabilized by rapeseed proteins. *Foods, 10*(7), 1657.
Petker, K., Rogers, M. A., & Joye, I. J. (2021). Chemical hardening of gliadin nanoparticles alters their oil-water interfacial behaviour. *Food Structure, 30*, Article 100218.
Rashidinejad, A., Birch, E. J., Sun-Waterhouse, D., & Everett, D. W. (2014). Delivery of green tea catechin and epigallocatechin gallate in liposomes incorporated into low-fat hard cheese. *Food Chemistry, 156*, 176–183.
Ren, Z., Chen, Z., Zhang, Y., Lin, X., Li, Z., Weng, W., … Li, B. (2021). Effect of heat-treated tea water-insoluble protein nanoparticles on the characteristics of Pickering emulsions. *LWT, 149*, Article 111999.
Rezvani, M., Manca, M. L., Muntoni, A., De Gioannis, G., Pedraz, J. L., Gutierrez, G., … Manconi, M. (2022). From process effluents to intestinal health promotion: Developing biopolymer-whey liposomes loaded with gingerol to heal intestinal wounds and neutralize oxidative stress. *International Journal of Pharmaceutics, 613*, Article 121389.
Sáez-Orviz, S., Marcet, I., Rendueles, M., & Díaz, M. (2022). Preparation of Edible Films with Lactobacillus plantarum and Lactobionic Acid Produced by Sweet Whey Fermentation. *Membranes, 12*(2), 115.
Sassi, C. B., Marcet, I., Rendueles, M., Díaz, M., & Fattouch, S. (2020). Egg yolk protein as a novel wall material used together with gum Arabic to encapsulate polyphenols extracted from Phoenix dactylifera L pits. *LWT, 131*, Article 109778.
Sharkawy, A., Barreiro, M. F., & Rodrigues, A. E. (2021). New Pickering emulsions stabilized with chitosan/collagen peptides nanoparticles: Synthesis, characterization and tracking of the nanoparticles after skin application. *Colloids and Surfaces A: Physicochemical and Engineering Aspects, 616*, Article 126327.
Sow, L. C., Chong, J. M. N., Liao, Q. X., & Yang, H. (2018). Effects of κ-carrageenan on the structure and rheological properties of fish gelatin. *Journal of Food Engineering, 239*, 92–103.
Tarhini, M., Greige-Gerges, H., & Elaissari, A. (2017). Protein-based nanoparticles: From preparation to encapsulation of active molecules. *International Journal of Pharmaceutics, 522*(1–2), 172–197.
Tcholakova, S., Denkov, N. D., Sidzhakova, D., Ivanov, I. B., & Campbell, B. (2003). Interrelation between drop size and protein adsorption at various emulsification conditions. *Langmuir, 19*(14), 5640–5649.
Wang, A., Xiao, Z., Wang, J., Li, G., & Wang, L. (2020). Fabrication and characterization of emulsion stabilized by table egg-yolk granules at different pH levels. *Journal of the Science of Food and Agriculture, 100*(4), 1470–1478.
Wang, H., Yao, L., & Wang, T. (2014). Extraction of phospholipids from structured dry egg yolk. *Journal of the American Oil Chemists' Society, 91*(3), 513–520.
Xiao, J., Gonzalez, A. J. P., & Huang, Q. (2016). Kafirin nanoparticles-stabilized Pickering emulsions: Microstructure and rheological behavior. *Food Hydrocolloids, 54*, 30–39.
Yang, H., Su, Z., Meng, X., Zhang, X., Kennedy, J. F., & Liu, B. (2020). Fabrication and characterization of Pickering emulsion stabilized by soy protein isolate-chitosan nanoparticles. *Carbohydrate Polymers, 247*, Article 116712.
Yue, M., Huang, M., Zhu, Z., Huang, T., & Huang, M. (2022). Effect of ultrasound assisted emulsification in the production of Pickering emulsion formulated with chitosan self-assembled particles: Stability, macro, and micro rheological properties. *LWT, 154*, Article 112595.
Zhang, T., Xu, J., Chen, J., Wang, Z., Wang, X., & Zhong, J. (2021). Protein nanoparticles for Pickering emulsions: A comprehensive review on their shapes, preparation methods, and modification methods. *Trends in Food Science & Technology, 113*, 26–41.
Zhang, Y., Chen, Y., Xiong, Y., Ding, B., Li, Z., & Luo, Y. (2022). Preparation of high internal phase pickering emulsions stabilized by egg yolk high density lipoprotein: Stabilizing mechanism under different pH values and protein concentrations. *LWT*, Article 113091.
Zhao, M., Shen, P., Zhang, Y., Zhong, M., Zhao, Q., & Zhou, F. (2021). Fabrication of soy protein nanoparticles via partial enzymatic hydrolysis and their role in controlling lipid digestion of oil-in-water emulsions. *ACS Food Science & Technology, 1*(2), 193–204.
Zhu, Y. Q., Chen, X., McClements, D. J., Zou, L., & Liu, W. (2018). Pickering-stabilized emulsion gels fabricated from wheat protein nanoparticles: Effect of pH, NaCl and oil content. *Journal of Dispersion Science and Technology, 39*(6), 826–835.